

This is a repository copy of *Effects of Methyl Branching on the Properties and Performance of Furandioate-Adipate Copolyesters of Bio-Based Secondary Diols*.

White Rose Research Online URL for this paper:

<https://eprints.whiterose.ac.uk/167588/>

Version: Published Version

---

**Article:**

Little, Alastair, Pellis, Alessandro, Comerford, James William orcid.org/0000-0002-9977-5695 et al. (4 more authors) (2020) Effects of Methyl Branching on the Properties and Performance of Furandioate-Adipate Copolyesters of Bio-Based Secondary Diols. ACS Sustainable Chemistry & Engineering. 14471–14483. ISSN 2168-0485

<https://doi.org/10.1021/acssuschemeng.0c04513>

---

**Reuse**

This article is distributed under the terms of the Creative Commons Attribution (CC BY) licence. This licence allows you to distribute, remix, tweak, and build upon the work, even commercially, as long as you credit the authors for the original work. More information and the full terms of the licence here:

<https://creativecommons.org/licenses/>

**Takedown**

If you consider content in White Rose Research Online to be in breach of UK law, please notify us by emailing [eprints@whiterose.ac.uk](mailto:eprints@whiterose.ac.uk) including the URL of the record and the reason for the withdrawal request.

## Effects of Methyl Branching on the Properties and Performance of Furandioate-Adipate Copolyesters of Bio-Based Secondary Diols

Alastair Little, Alessandro Pellis, James W. Comerford, Edwin Naranjo-Valles, Nema Hafezi, Mark Mascall,\* and Thomas J. Farmer\*

Cite This: *ACS Sustainable Chem. Eng.* 2020, 8, 14471–14483

Read Online

ACCESS |



Metrics &amp; More



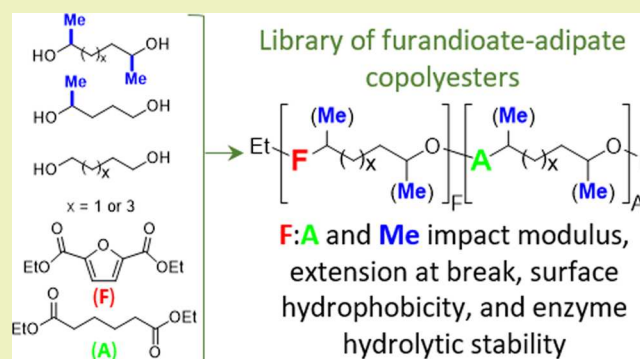
Article Recommendations



Supporting Information

**ABSTRACT:** Furandioate-adipate copolyesters are an emerging class of bio-based biodegradable polymers with great potential to replace fossil-derived terephthalic acid-based copolyesters such as poly(butylene adipate-co-terephthalate) (PBAT). Furandioate-adipate polyesters have almost exclusively been prepared with conventional primary ( $1^\circ$ ) alcohol diols, while secondary ( $2^\circ$ ) alcohol diol monomers have largely been overlooked until now, despite preliminary observations that using methyl-branched diols increases the  $T_g$  of the resultant polyesters. Little is known of what impact the use of  $2^\circ$  alcohol diols has on other properties such as material strength, hydrophobicity, and rate of enzymatic hydrolysis—all key parameters for performance and end-of-life. To ascertain the effects of using  $2^\circ$  diols on the properties of furandioate-adipate copolyesters, a series of polymers from diethyl adipate (DEA) and 2,5-furandicarboxylic acid diethyl ester (FDEE) using different  $1^\circ$  and  $2^\circ$  alcohol diols was prepared. Longer transesterification times and greater excesses of diol (diol/diester molar ratio of 2:1) were found to be necessary to achieve  $M_w$ s  $> 20$  kDa using  $2^\circ$  alcohol diols. All copolyesters from  $2^\circ$  diols were entirely amorphous and exhibited higher  $T_g$ s than their linear equivalents from  $1^\circ$  diols. Compared to linear poly(1,4-butylenedipate-co-1,4-butylenefurandioate), methyl-branched, poly(2,5-hexamethylenedipate-co-2,5-hexamethylenefurandioate) (0.7:0.3 furandioate/adipate ratio) displayed both higher modulus (67.8 vs 19.1 MPa) and higher extension at break (89.7 vs 44.5 mm). All other methyl-branched copolyesters displayed lower modulus but retained higher extension at break compared with their linear analogues. Enzymatic hydrolysis studies using *Humicola insolens* cutinase revealed that copolyesters from  $2^\circ$  alcohol diols have significantly decreased rates of biodegradation than their linear equivalents synthesized using  $1^\circ$  alcohol diols, allowing for fine-tuning of polymer stability. Hydrophobicity, as revealed by water contact angles, was also found to generally increase through the introduction of methyl branching, demonstrating potential for these materials in coatings applications.

**KEYWORDS:** bio-based polymers, 5-(chloromethyl)furfural, adipic acid, secondary alcohol diols, 2,5-furandicarboxylic acid



## INTRODUCTION

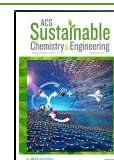
Wu and Arnaud *et al.* reported in 2016 and 2017 the synthesis of a series of novel polyesters from secondary ( $2^\circ$ ) diol monomers derived from 5-(chloromethyl)furfural (CMF), a platform molecule obtainable in high yields directly from the polysaccharides in biomass.<sup>1,2</sup> Various “methyl-branched” polyesters were synthesized from 2,3-butanediol (2,3-BDO), 2,5-hexanediol (2,5-HDO), 2,7-octanediol (2,7-ODO), diethyl adipate (DEA), and 2,5-furandicarboxylic acid diethyl ester (FDEE) *via* polycondensation. The resultant polymers were characterized by nuclear magnetic resonance (NMR) spectroscopy, gel permeation chromatography (GPC), and differential scanning calorimetry (DSC), demonstrating the potential to produce copolyesters effectively. Scheme 1 shows the common derivation of 2,5-HDO, 2,7-ODO, DEA, and FDEE from CMF. Thus, a trifurcated route starting at CMF leads either toward the rehydration product levulinic

acid (path *a*),<sup>3</sup> oxidation to 2,5-diformylfuran (path *f*),<sup>4</sup> or reduction to 2,5-dimethylfuran (path *i*).<sup>5</sup> The pathways are broken out in detail in the Scheme itself but, in general, routes *a*  $\rightarrow$  *c* and *a*  $\rightarrow$  *e* involve Kolbe-type electrochemical syntheses of DEA and 2,7-ODO,<sup>2,6,7</sup> while *f*  $\rightarrow$  *h* and *i*  $\rightarrow$  *k* comprise the oxidation of CMF ultimately to FDEE or hydrolysis of 2,5-dimethylfuran and reduction of the resulting dione to 2,5-HDO, respectively.<sup>8–10</sup> The longer chain diol 2,7-ODO was found to be the most reactive of the series, giving rise to higher molecular weight ( $M_w$ ) materials, because of comparatively

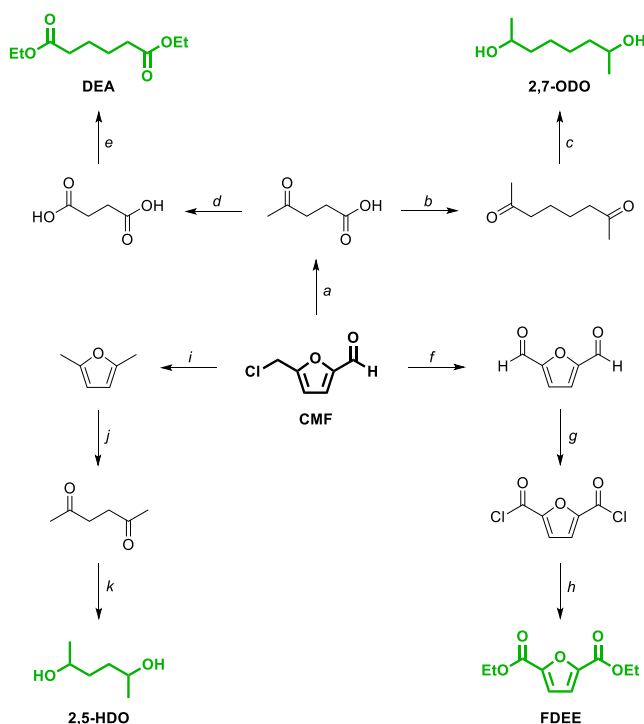
Received: June 22, 2020

Revised: August 12, 2020

Published: September 4, 2020



### Scheme 1. CMF as a Common Platform for Accessing Diacids and Branched Diols Used in This Study



(a)  $\text{H}_2\text{O}$ ,  $\Delta$ ;<sup>3</sup> (b)  $-\text{e}^-$ , KOH, MeOH;<sup>2</sup> (c)  $\text{H}_2$ , Pd/C;<sup>2</sup> (d)  $\text{H}_2\text{O}_2$ , TFA;<sup>6</sup> (e) monoesterification, then  $-\text{e}^-$ , MeOH– $\text{H}_2\text{O}$ ; (f) DMSO,  $\Delta$ ; (g)  $t\text{-BuOCl}$ ; (h) EtOH;<sup>8</sup> (i) BuOH, HCl, then  $\text{H}_2$ , Pd/C;<sup>5</sup> (j)  $\text{H}_2\text{O}$ ,  $\text{H}^+$ ; (k)  $\text{H}_2$ , Ru cat,  $\text{H}_2\text{O}$ .<sup>10,12</sup>

lower steric hindrance and suppression of side reactions (e.g., dehydration to form a cyclic ether) relative to other diols in the series. The presence of methyl branches increases steric interactions between chains and reduces chain flexibility, resulting in increased glass-transition temperatures ( $T_g$ s) compared to equivalent polymers produced using primary ( $1^\circ$ ) alcohol diols.<sup>1,2</sup> This relationship has been studied in detail by DiStasio *et al.* for a series of phthalic anhydride polyesters with increasing degrees of methyl branching on the phthalate ring but not the diol. DiStasio likewise concluded that the addition of methyl groups introduced greater steric strain and thus increased  $T_g$ , though these groups will also likely alter other properties such as end-group composition, crystallinity, and surface energy.<sup>11</sup>

Arnaud and Boyd, in separate studies, also observed similar trends in degrees of crystallinity: polyesters of the  $1^\circ$  alcohol diol 1,6-HDO were highly crystalline ( $\sim 60\%$ ), whereas 2,5-HDO polyesters were entirely amorphous (no melting temperature observed).<sup>1,13</sup> In these studies, the 2,5-HDO diol was a mixture of stereoisomers, thus it was assumed that the stereo-irregularity disrupted the crystal packing of the polyesters, contributing to their amorphous behavior. This was later confirmed by van der Klis *et al.*, who found a polyester of optically pure 2,5-HDO, poly(2*S*,5*S*-hexylene succinate) to display a melting point ( $T_m$ ) at 200  $^\circ\text{C}$ , confirming it to be semicrystalline.<sup>14</sup> The thermal stability of the polyesters in these earlier studies was also promising. Arnaud and co-workers showed their materials to have temperatures of decomposition with 10% mass loss ( $\text{TD}_{10}$ ) to be  $>280^\circ\text{C}$ ,

while van der Klis found  $\text{TD}_{10}$  to be  $>250^\circ\text{C}$  for all 2,5-HDO polyesters they prepared.

Polyesters from these  $2^\circ$  alcohol diols can be considered to be “methyl-branched” analogues of polyesters from  $1^\circ$  alcohol diols with the same hydroxyl group relationship but containing two fewer carbons along the backbone. 2,5-HDO is thus a methyl-branched analogue of 1,4-butanediol (1,4-BDO), and 2,7-octanediol (2,7-ODO) is a methyl-branched analogue of 1,6-HDO (Figure 1). van der Klis *et al.* have preliminarily

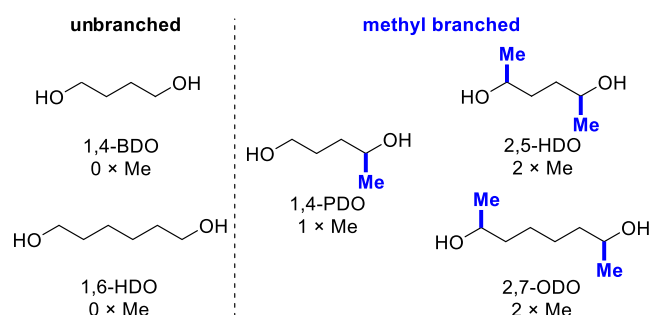


**Figure 1.** Diols used in this study with methyl branches highlighted in blue.

examined this relationship in homopolymers of 1,4-BDO, 1,4-pentanediol (1,4-PDO), and 2,5-HDO as diols containing 0, 1, and 2 methyl branches per monomer, respectively, with succinic acid, adipic acid, and 2,5-furandicarboxylic acids.<sup>14</sup> The addition of methyl branches was found to reduce polymer crystallinity, linked as noted above to the use of stereo-irregular diols. Interestingly, the introduction of methyl branching raised the  $T_g$  of the amorphous regions of these materials, though multiple factors are known to affect  $T_g$  beyond just sterics. For example, increasing the surface area due to additional carbons in the diols will lead to more chain–chain interaction, while the free volume between the chains of the materials will also alter across the series.

However, the influence of methyl branching on the biodegradability, mechanical properties, and hydrophobicity of this family of bio-based polyesters is yet to be examined. Bio-based  $2^\circ$  alcohol-containing monomers are not a new concept in polymer chemistry; for example, lactic acid, 2,3-BDO, and isosorbide are all well-established materials. Poly(lactic acid) (PLA) requires ring-opening polymerization of lactide to access high  $M_w$ , with condensation and transesterification of LA directly resulting only in oligomers. Although a diverse range of applications are known for PLA, it is also widely recognized that its material performance is nonideal in some instances, and especially the hydrophilicity of its polyesters (native contact angle of  $72^\circ$ ) negatively impacts serviceability in some cases.<sup>15</sup> For example, the surface of PLA must be modified to make it suitable for applications such as no mass loss droplet transport<sup>15,16</sup> or reduced water ingress in crop net protection.<sup>17</sup> However, these modification protocols can be laborious and require the use of various solvents and coagulants, while also being heavily influenced by the crystallinity of the PLA surface.<sup>18</sup> 2,3-BDO is the simplest  $2^\circ$  alcohol-containing diol, though it regularly gives low-chain length polyesters when combined with aromatic diacids under transesterification conditions.<sup>1,19,20</sup> Isosorbide polyesters are widely studied, and this diol increases the  $T_g$  and thermal stability of the resultant materials, but also suffers from sluggish

kinetics with the added complication that reactivity differs between the two hydroxyl groups.<sup>21–23</sup>

Polyester mechanical performance can be improved by the incorporation of rigid groups in the backbone, with furan diacids being one of the most investigated bio-based options in recent times. However, there is very little literature surrounding the effects of methyl branching on the hydrophobicity, mechanical performance, and hydrolytic stability of furandioate polymers. When researching the rates of enzymatic hydrolysis of furandioate polyesters, Haernvall *et al.* detected a fourfold increase in enzyme activity when 1,3-propanediol was replaced by its branched analogue, 1,2-propanediol, but the molecular weights of the polymers and their respective  $T_g$ s were significantly different.<sup>24</sup> On the other hand, Ejlertsson *et al.* reported that using branched alcohols to synthesize phthalic acid esters (PVC plasticizers) decreases their enzymatic hydrolysis rates.<sup>25</sup>

In comparison to poly(1,3-propylene 2,5-furandioate) (PPF), Genovese *et al.* found the methyl-branched poly(neopentyl glycol 2,5-furandioate) to be more hydrophobic, have higher  $T_g$  and  $T_m$ , higher elastic modulus ( $E$ ), higher stress at break ( $\sigma_b$ ), and a similar extension at break ( $\epsilon_b$ ).<sup>26</sup> Subsequently, Guidotti *et al.* studied a family of poly(butylene/neopentyl 1,4-cyclohexane dicarboxylate) copolyesters containing butylene-cyclohexane and neopentyl-cyclohexane units where their ratio was used to tune the polymer properties.<sup>27</sup> Here, the methyl branches of the neopentyl moiety disrupted the formation of ordered phases, enhancing the polymer's flexibility (increasing  $\epsilon_b$ ), but decreasing its  $E$  and  $\sigma_b$ , with respect to analogous polyesters with no methyl branching. These researchers used the same technique to enhance the flexibility of PBS.<sup>27</sup>

Thus, we recognized that methyl branching could be used to the same effect in linear furandioate-adipate copolyesters, enhancing mechanical performance that could be of value for further commercialization of materials such as the biodegradable film-forming polyester poly(1,4-butylene adipate-co-1,4-butylene 2,5-furandioate) (1,4-PBAF) as well as in coatings.<sup>28,29</sup> A challenge remains as to how mechanical performance and hydrolytic resistance can be tuned independent of crystallinity. Innovative bio-based monomers that use methyl branching to enable this kind of control may be of strong commercial interest, particularly in the field of surfaces and coatings where combined hydrophobic control, thermal and hydrolytic stability, and mechanical strength are desirable characteristics.<sup>30,31</sup>

Herein is described a comprehensive evaluation of the mechanical properties, enzyme-catalyzed hydrolysis, and surface hydrophobicity of methyl-branched furandioate-adipate copolyesters (Figure 2) using the aforementioned 2° alcohol diols 1,4-PDO, 2,5-HDO, and 2,7-ODO. A comparison is made with the corresponding linear (i.e., unbranched) 1° alcohol diols 1,4-BDO and 1,6-HDO. Of particular importance was the determination of the correct copolymer composition that produced materials capable of being formed into films, where a careful balance between the rigid furan diacid and the more flexible adipate unit would be key to success.

## RESULTS AND DISCUSSION

It has previously been reported that the thermomechanical properties and  $T_g$  of aliphatic-aromatic copolyesters improve with increasing fraction of aromatic units.<sup>29,32</sup> Although high mechanical strength is often desirable, too much rigid aromatic

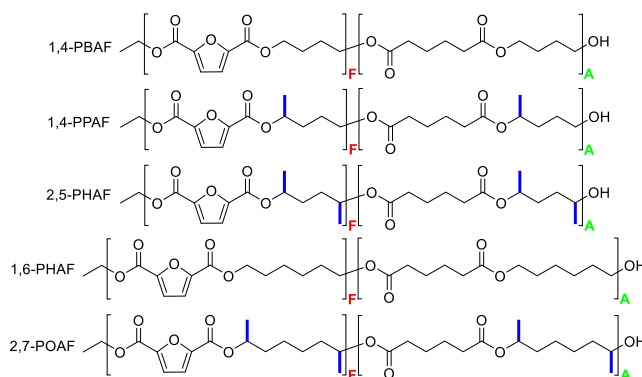
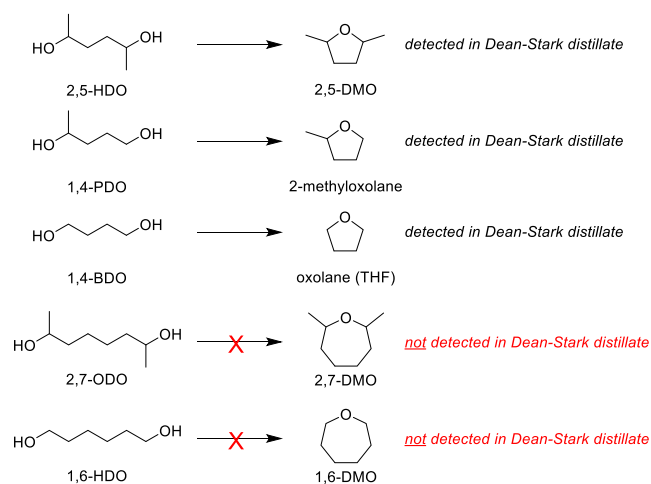


**Figure 2.** Adipate-co-2,5-furandioate polyesters with methyl branches highlighted in blue. From top to bottom: poly(1,4-butylene adipate-co-1,4-butylene 2,5-furandioate) (1,4-PBAF), poly(1,4-pentylene adipate-co-1,4-pentylene 2,5-furandioate) (1,4-PPAF), poly(2,5-hexylene adipate-co-2,5-hexylene 2,5-furandioate) (2,5-PHAF), poly(1,6-hexylene adipate-co-1,6-hexylene 2,5-furandioate) (1,6-PHAF), and poly(2,7-octylene adipate-co-2,7-octylene 2,5-furandioate) (2,7-POAF), where “red F” is the furandioate unit and “green A” is the adipate unit. All polyesters were random copolymers.

content can hinder the processability of polyesters, causing issues in film formation, injection molding, and coating preparation. Thus, in order to achieve a material that was firm enough for mechanical testing, yet soft enough to be melt-processed into a film, a benchmarking series of 2,5-PHAF copolyesters of varying furandioate/total diester molar ratios ( $F/D$ , where  $F$  = number of furandioate units;  $D$  = furandioate + adipate, i.e., total number of diester units) were initially synthesized (see the Supporting Information, Table S1). All polyesters in this preliminary screening were of low  $M_n$  (<4.2 kDa), other than the poly(2,5-hexylene adipate) (2,5-PHA) homopolymer (25 kDa). Visual inspection of the materials indicated that an  $F/D \geq 0.6$  is required to produce materials that were not tacky and rigid enough for film formation. During this initial screening, 2,5-dimethyloxolane (2,5-DMO, Scheme 2) was observed in the Dean–Stark trap, suggesting that some 2,5-HDO was dehydrated to this volatile cyclic ether. Sullivan *et al.* previously showed that this reaction occurs

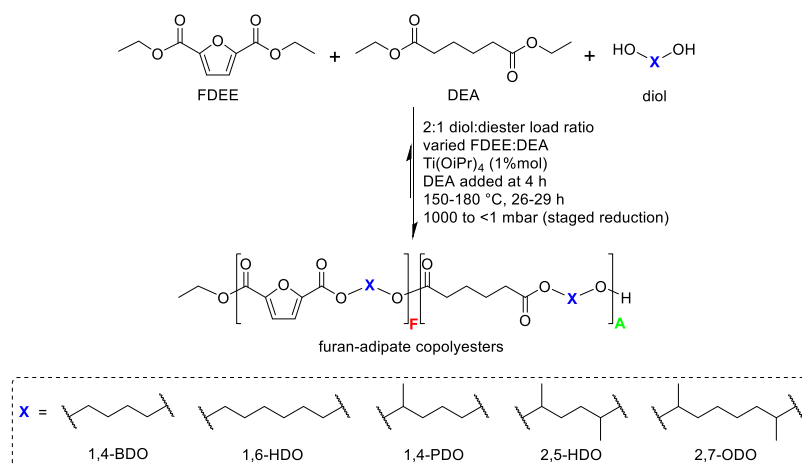
## Scheme 2. Cyclic Ether Formation from Diols



Dean–Stark distillate was recovered and analyzed by  $^1\text{H}$  NMR spectroscopy (Supporting Information, Section S2).



Scheme 3. Random Copolyesters from Diethyl 2,5-Furandioate (FDEE), Diethyl Adipate (DEA), and Various Diols

Table 1. Number-Average Molecular Weight ( $M_n$ ), Weight-Average Molecular Weight ( $M_w$ ), Dispersity ( $\bar{D}$ ), Furandioate to Total Diester Molar Fraction ( $F/D$ ), End-Group Ratio (%  $-\text{OH}$ ), Glass-Transition Temperature ( $T_g$ ), and Melting Temperature ( $T_m$ ) of the Isolated Polyesters

entry	polymer	$M_n^a$ /kDa	$M_w^a$ /kDa	$\bar{D}^a$	$F/D^c$	% $-\text{OH}$ end groups <sup>b</sup>	$T_g^e$ /°C	$T_m^e$ /°C
1	1,4-PBA	31 (20 <sup>b</sup> )	63	2	0	100 <sup>d</sup>	−68	56 {47}
2	1,4-PBAF0.5	18 (9.3 <sup>b</sup> )	28	1.6	0.51	100 <sup>d</sup>	−26	91 {nd}
3	1,4-PBAF0.6	6.5 <sup>b</sup>	Nd	Nd	0.61	100 <sup>d</sup>	−23	113 {25}
4	1,4-PBAF0.7	10 <sup>b</sup>	Nd	Nd	0.69	100 <sup>d</sup>	−13	132 {21}
5	1,4-PBF	nd <sup>+</sup>	nd <sup>+</sup>	nd <sup>+</sup>	nd <sup>+</sup>	15*	15*	170 {46}
6	1,4-PPA	22 (9.3 <sup>b</sup> )	37	1.7	0	100 <sup>d</sup>	−50	‡
7	1,4-PPAF0.5	19 (9.5 <sup>b</sup> )	34	1.8	0.52	100 <sup>d</sup>	−10	‡
8	1,4-PPAF0.6	17 (7.1 <sup>b</sup> )	29	1.6	0.58	100 <sup>d</sup>	−3	‡
9	1,4-PPAF0.7	21 (23 <sup>b</sup> )	37	1.8	0.70	100 <sup>d</sup>	12	‡
10	1,4-PPF	1.7 (nd <sup>#</sup> )	2.9	1.7	1	nd <sup>#</sup>	22	‡
11	2,5-PHA	27 (11 <sup>b</sup> )	45	1.6	0	100 <sup>d</sup>	−34	‡
12	2,5-PHAF0.5	16 (6.7 <sup>b</sup> )	24	1.5	0.49	38 [48]	0	‡
13	2,5-PHAF0.6	23 (13 <sup>b</sup> )	34	1.5	0.61	100 <sup>d</sup>	19	‡
14	2,5-PHAF0.7	15 (6.8 <sup>b</sup> )	22	1.5	0.71	100 <sup>d</sup>	27	‡
15	2,5-PHF	3.4 (2.0 <sup>b</sup> )	5.9	1.7	1	91 [100]	37	‡
16	1,6-PHA	23 (7.6 <sup>b</sup> )	39	1.7	0	100 <sup>d</sup>	‡	57 {70}
17	1,6-PHAF0.5	3.2 <sup>b</sup>	Nd	nd	0.51	100 <sup>d</sup>	−66	80 {19}
18	1,6-PHAF0.6	4.2 <sup>b</sup>	Nd	nd	0.63	100 <sup>d</sup>	−37	97 {22}
19	1,6-PHAF0.7	6.8 <sup>b</sup>	Nd	nd	0.72	100 <sup>d</sup>	−25	80 {25}
20	1,6-PHF	2.8 <sup>b</sup>	Nd	nd	1	100 <sup>d</sup>	4	143 {58}
22	2,7-POA	21 (6.4 <sup>b</sup> )	110	5.3	0	72 [0]	−42	‡
23	2,7-POAF0.5	17 (4.8 <sup>b</sup> )	57	3.5	0.51	79 [48]	−7	‡
24	2,7-POAF0.6	11 (3.6 <sup>b</sup> )	39	2.9	0.61	100 <sup>d</sup>	−1	‡
25	2,7-POAF0.7	9.5 (2.6 <sup>b</sup> )	21	2.9	0.71	88 [64]	4	‡
26	2,7-POF	18 (5.4 <sup>b</sup> )	45	2.5	1	80 [100]	39	‡

<sup>a</sup>Determined by GPC. <sup>b</sup>Determined by end-group analysis using <sup>1</sup>H NMR. Value in parentheses ( ) is additional  $M_n$  determined by end-group analysis using <sup>1</sup>H NMR. <sup>c</sup>Determined by <sup>1</sup>H NMR.  $F/D$  = furandioate molar fraction relative to the total diester.  $D$  = total diester molar fraction ( $F$  plus adipate,  $A$ ). <sup>d</sup>Only hydroxyl end groups were detected, possibly with ethyl ester signals obscured by constitutional repeat units (CRUs), see Supporting Information section S3. [ ] value in brackets is % of ester end groups that are furandioate (~4.4 ppm), as opposed to adipate (~4.1 ppm). <sup>e</sup>Determined by modulated DSC. \*: DSC data showing the sample having a very low intensity  $T_g$  trace. nd: Not determined as the sample was insoluble in THF. nd<sup>+</sup>: Not determined as the sample was insoluble in  $\text{CDCl}_3$ . nd<sup>#</sup>: not determined as end groups were obscured in NMR spectra. Value in braces { } is enthalpy of fusion (melt) in J/g, as determined by integration of the endothermic peak(s). ‡: No thermal transition was observed. Comparative results from other studies in the literature are given in Table S8 of the Supporting Information. Details of optimized polymerization conditions, including  $F/D$  feed ratios and time of adipate addition, are described in the Materials and Methods section and Table 4.

easily under acidic conditions.<sup>12</sup> Wu *et al.* found oxolane (THF) formation from 1,4-BDO under polycondensation conditions,<sup>33</sup> and we likewise observed cyclic ether formation both for this diol and 1,4-PDO, but not for 1,6-HDO or 2,7-ODO (Scheme 3, Section S2). 2,5-PHAF0.7 ( $F/D = 0.7$ ) was

selected as the target polyester to optimize 2° alcohol diol polymerization via a catalyst screening (Section S12) and variation in reaction conditions (Section S13). This polymer was chosen as it produced a tough, yet flexible, nonsticky material, while higher incorporation of FDEE was found to

result in materials that were too brittle. From the catalyst screening, both  $\text{Ti}(\text{OiPr})_4$  and  $\text{Sb}_2\text{O}_3$  were found to be superior to other catalysts tested (Table S2), and the former was ultimately selected over the latter on the basis of elemental sustainability (Table S3) and toxicity (Table S4) considerations.<sup>34</sup> When optimizing the synthesis of poly(1,4-butylene furandioate) (1,4-PBF), Zhu *et al.* found that keeping the reaction temperature 30 °C below the boiling point of BDO (230 °C) yielded a maximum  $M_w$ .<sup>35</sup> 2,5-HDO has a boiling point of 216–218 °C, therefore, in agreement with Zhu's recommendation, all our experiments were performed between 150 and 180 °C. Ultimately, it was found that the best way to improve chain length in the furandioate-adipate copolyesters was to use a 2:1 ratio of diol to total diester and to add the faster reacting DEA after 4 h, thus allowing the furandioate bisdiol to initially form (Tables S7), an approach similar to that previously used in the synthesis of itaconate polyesters.<sup>36</sup>

Furandioate-adipate copolyesters using the 2° alcohol-containing diols 1,4-PDO, 2,5-HDO, and 2,7-ODO were subsequently synthesized applying the optimized conditions for 2° alcohols determined from the preliminary screening above. Full details for the optimized conditions are given in the Materials and Methods section. For each, the molar fraction of *F* relative to total diacid ( $D = F + A$ ) was varied over the range of 0 (adipate only), 0.5, 0.6, 0.7 to 1 (furandioate only). The 1° alcohol diol equivalent polyesters were prepared from 1,4-BDO and 1,6-HDO using 1° alcohol conditions, which differ from the 2° alcohol conditions by the earlier addition of adipate (2 h rather than 4 h), and for 1,6-HDO, a lower molar excess of diol was possible (1.25:1 for 1,6-HDO as opposed to 2:1 for all other polymers).

## MOLECULAR MASS AND THERMAL PROPERTIES OF POLYESTERS

The polyesters that resulted from using the optimized reaction conditions were initially analyzed by GPC and DSC (Table 1). 1,4-PBAF0.6–0.7, 1,4-PBF, 1,6-PHAF0.5–0.7, and 1,6-PHF were insoluble in the GPC solvent (THF), so for these polymers,  $M_n$  values were calculated using end-group analysis by  $^1\text{H}$  NMR. Where possible, end-group analysis is also given for those polymers analyzed by GPC, showing a general trend of GPC values being approximately double those estimated by NMR spectroscopy. Examples of these calculations are shown in the Supporting Information (Section S3).

1,4-PBAFs and their methyl-branched equivalents (2,5-PBAFs) all show similar  $M_n$ ,  $M_w$ , and dispersity ( $\bar{D}$ ) values. GPC traces (Supporting Information, Section S4) of all the polyesters with  $F/D \leq 0.7$  in Table 1 showed broad monomodal distributions. Polyesters 1,4-PPF and 2,5-PHF contained many low molecular weight oligomer peaks, reflecting the lower degrees of polymerization in furandioate-only polyesters. In contrast to this, the GPC peaks from the 2,7-POAF polymers were very broad (Figure S34), which is reflected in their large  $\bar{D}$  values. The same polymers synthesized by Arnaud showed much lower  $\bar{D}$  values (all <2.1, Table S8).<sup>1</sup> Despite their high  $M_w$  (>22 kDa), the fully aliphatic polyesters 1,4-PPA, 2,5-PHA, and 2,7-POA were all tacky gums, confirming the necessity to prepare copolyesters with aromatic units to obtain rigid film-forming materials. As was found by Arnaud *et al.*, the  $M_w$ s of the 2,7-POAF polymers were generally higher than those of the 2,5-PHAF polymers, which can be mainly attributed to reduced steric influence and

the absence of oxepane formation as a side reaction (cf. Scheme 2), an issue that was observed for 2,5-HDO and 1,4-BDO (Supporting Information, Section S2).  $^1\text{H}$  NMR analysis (Supporting Information, Section S3) confirmed that the feed molar fraction of furandioate to total diester was maintained in the final isolated polyesters (*F/D*, Table 1). The percentage of hydroxyl end groups (% –OH) was also determined by NMR analysis, though this analysis was not possible for the 1° alcohol diol polyesters as the ethyl ester  $\text{CH}_2$  signals (4.4 and 4.1 ppm for furan and adipate end groups, respectively) were obscured by the main polymer chain signals. The 2,5-HDO series of polyesters generally have hydroxyl-only end groups, the exceptions being 2,5-PHAF0.5 (38% hydroxyl end group) and 2,5-PHF (91%). The 2,7-ODO series showed a higher fraction of ester end groups.

As shown by Figure 3, all the polymers, as expected, show an increase in  $T_g$  with increasing furandioate unit content. The

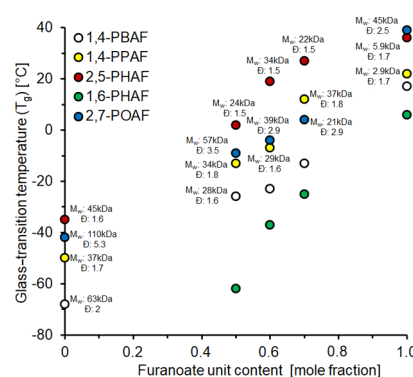


**Figure 3.** Glass-transition temperature ( $T_g$ ) of 1,4-PBAF, 1,4-PPAF, 2,5-PHAF, 1,6-PHAF, and 2,7-POAF, as determined by DSC (traces shown in the Supporting Information, Section S6).  $M_w$  and  $\bar{D}$ , as determined by GPC, are shown for each sample where data are available.

polymers also show a decrease in  $T_g$  with increasing diol chain length, representing higher chain mobility for longer diols. Methyl branching was shown to raise the  $T_g$  because of a reduction in chain flexibility. However, as these polymers vary in  $M_w$  and  $T_g$  typically increases with  $M_w$ , these trends in  $T_g$  are not wholly representative of the effects of changing the polymers' structures. For example, the 2,7-ODO diol unit imparts greater chain flexibility in comparison to 2,5-HDO, causing the 2,7-POAF series to have lower  $T_g$ s than the equivalent 2,5-PHAF series. However, as the  $M_w$  of 2,7-POF is ~8 times greater than that of 2,5-PHF, it has a higher observed  $T_g$  in this dataset. Melting points ( $T_m$ ) were only observed in polyesters made using 1° alcohol diols (1,4-BDO and 1,6-HDO series), highlighting the semicrystalline nature of these polymers versus the 2° alcohol diol alternatives. Using the enthalpy of crystallization as a crude measure of the degree of crystallinity, it can be observed that the homopolymers of either adipate or furandioate with 1,4-BDO and 1,6-HDO are more crystalline than the copolymers. Across the 1,6-HDO copolyester series, there is an indication that the degree of crystallinity increases slightly as  $F/D$  increases from 0.5 through 0.7, though the same trend is not seen for the 1,4-BDO series.

$T_g$  values of 2,5-PHAF0.5 and 2,7-POAF0.5 are comparable to those reported by Arnaud, despite the polymers synthesized in this study having a higher  $M_w$ . 2,5-PHA and 1,4-PPA

**Table 2.** Modulus, Stress at Break ( $\sigma_b$ ), Extension at Break ( $\epsilon_b$ ), Strain at Break, and Maximum Load of Copolymers from Each Series

entry	polymer	$M_w^c$ /kDa ( $\bar{D}$ )	modulus/MPa	$\sigma_b$ /MPa	$\epsilon_b$ /mm	strain at break/mm/mm	max load/N
1	1,4-PBAF0.6	6.5 <sup>d</sup>	17.8 ± 1.0	4.79 ± 0.69	12.6 ± 4.6	0.63 ± 0.23	4.24 ± 0.60
2	1,4-PBAF0.7	10 <sup>d</sup>	19.1 ± 0.9	7.00 ± 0.21	44.5 ± 6.0	2.23 ± 0.30	6.30 ± 0.19
3 <sup>a</sup>	1,4-PPAF0.7	37 (1.8)	0.41 ± 0.02	0.69 ± 0.06	>500 ± 0	25.0 ± 0.0	0.62 ± 0.05
4 <sup>a</sup>	2,5-PHAF0.6	34 (1.5)	0.24 ± 0.09	0.69 ± 0.11	>500 ± 0	25.0 ± 0.0	0.62 ± 0.00
5	2,5-PHAF0.7	22 (1.5)	67.8 ± 11.1	4.15 ± 0.66	89.7 ± 47.9	4.48 ± 2.39	4.31 ± 0.76
6	2,5-PHAF0.7 <sup>b</sup>	17 (1.5)	41.4 ± 18.1	3.05 ± 0.55	203 ± 61	10.1 ± 3.1	2.89 ± 0.37
7	1,6-PHAF0.7	6.8 <sup>d</sup>	22.3 ± 5.0	5.61 ± 0.77	10.3 ± 4.0	0.52 ± 0.20	5.22 ± 0.72
8 <sup>a</sup>	2,7-POAF0.7	21 (2.9)	0.006 ± 0.006	0.01 ± 0.01	>500 ± 0.0	25.0 ± 0.00	0.006 ± 0.008

<sup>a</sup>Extension at break ( $\epsilon_b$ ) given as 500 mm, which is the limit of the machine. <sup>b</sup>2,5-PBAF0.7 was prepared using a lower diol excess compared to entry 5 (optimized synthesis), resulting in a polyester with lower  $M_n$  (12 kDa) and  $M_w$  (17 kDa). <sup>c</sup>Determined by GPC,  $\bar{D}$  given in parentheses, if known. <sup>d</sup>Determined by <sup>1</sup>H NMR end-group analysis, therefore they are  $M_n$  not  $M_w$ . Tensile experiment plots are presented in the [Supporting Information](#), Section S9.

synthesized under the conditions described here have  $M_w$  values more than double those previously reported by van der Klis *et al.* and Arnaud *et al.* and consequently show somewhat higher  $T_g$  values (−34 *vs* −39 °C and −50 *vs* −52 °C, respectively).<sup>1,14</sup> Literature data for 1,4-PBAFs and PHF are from higher  $M_w$  materials than those reported in this study; as a result, they have higher  $T_g$ s (Table S8).<sup>24,29</sup>

The tensile properties of these materials were then assessed at room temperature for polyesters where suitable films could be produced (Table 2). The adipate homopolymers, 1,4-PPA, 2,5-PHA, and 2,7-POA, were too soft and gum-like to undergo testing, and the furandioate homopolymers 1,4-PPF, 2,5-PHF, and 2,7-POF were too brittle to produce dumbbell-shaped samples. Despite their high  $M_w$ s, 1,4-PPAF0.5, 1,4-PPAF0.6, and 2,5-PHAF0.5 copolymers were too soft and deformable to be tested. Thus, tensile measurements were collected for all the copolymers with an  $F/D = 0.6$  or 0.7 (Figure 4).

The two 2,5-PHAF0.7 samples synthesized under different diol excesses (2:1 and 3:1 diol/diester, the diester being both FDEE and DEA at a ratio of 0.7:0.3) showed noticeable variation in their mechanical performance (Table 2, entries 5

and 6). These differences were attributed to a number of factors, the first being  $M_w$  with a lower modulus and  $\sigma_b$  (41.6 and 3.05 Mpa, respectively, for the 17 kDa polymer, entry 6) seen for the samples with a lower  $M_w$  compared with the better performing 2,5-PHAF0.7 (67.8 and 4.15 Mpa for the 22 kDa polymer, entry 5). However, tensile values for each 2,5-PHAF0.7 sample had high standard deviations (Figure 4). This was because not all runs of each sample came from the same film, so the thickness varied slightly. Because of their brittleness, the 2,5-PHAF0.7 films frequently broke while specimens were punched. These films were therefore first heated on a warmed Petri dish to raise their temperature above their  $T_g$  to make them soft enough to punch. This meant each sample was pressed and punched numerous times to obtain enough data points. The brittleness of the 2,5-PHAF0.7 films can be explained by the two methyl branches in the diol unit raising  $T_g$  (27 °C) to above room temperature. Indeed, this near room temperature  $T_g$  of entry 5 may also explain the lower mechanical performance for entry 6, where the drop in  $M_w$  subsequently caused a drop in  $T_g$  (19 °C) to below the temperature at which the measurements were performed. This does, however, highlight the potential that these 2° alcohol diol monomers give to tuning the polymer performance towards the range of being thermally responsive at room or body temperature.

2,5-PHAF0.7 displayed a superior modulus to 1,4-PBAF0.7 (67.8 and 19.1 Mpa, respectively), suggesting that the former is a stiffer material, again a clear effect of methyl branching. This is in agreement with the results of Genovese *et al.*, who observed that the methyl-branched poly(neopentyl furandioate) displayed a higher modulus than its linear analogue, poly(1,3-propyl furandioate).<sup>26</sup> 1,4-PBAF0.7 showed slightly higher  $\sigma_b$  than 2,5-PHAF0.7, demonstrating the former to be a stiffer material, which appears to be a result of its semicrystalline nature. Considering their brittleness and higher modulus, it was surprising to see that both 2,5-PHAF0.7s also displayed superior  $\epsilon_b$  to 1,4-PBAF0.7, suggesting better flexibility. The increased  $\epsilon_b$  of 2,5-PHAF0.7 could be explained by decreased crystallinity (no  $T_m$ ) compared to 1,4-PBAF0.7, indicating that the introduction of stereo-irregular methyl branching can improve processability when totally amorphous materials are desired. However, another plausible rationale is  $T_g$ , with 1,4-PBAF0.7 being in its rubbery state ( $T_g = -13$  °C), while 2,5-PHAF0.7 was in its glassy state (27 °C). The same trends were not observed in 2,5-PHAF0.6 and 1,4-PBAF0.6. Here, 2,5-PHAF0.6 displayed a much lower modulus and  $\sigma_b$ , but a higher

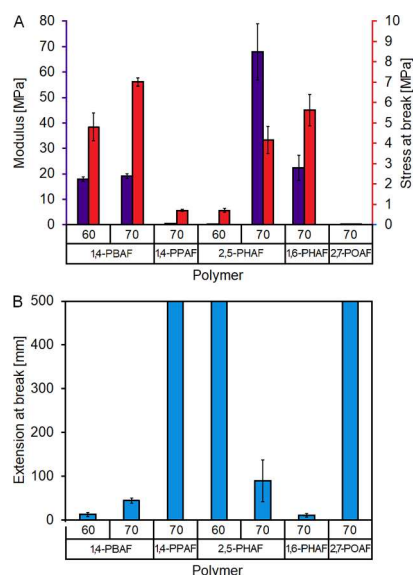


**Figure 4.** Tensile properties of materials. (A) Modulus and stress at break and (B) extension at break. Note that 1,4-PPAF0.7, 2,5-PHAF0.7 and 2,7-POAF0.7 did not break at the instrument's 500 mm maximum extension.



$\epsilon_b$  than 1,4-PBAF0.6, showing 2,5-PHAF0.6 to be more flexible than 1,4-PBAF0.6. In this study, 1,4-PBAF0.6 displayed a lower modulus, lower  $\sigma_b$ , and lower  $\epsilon_b$  than 1,4-PBAF0.7, while in previous studies, these two polymers exhibited a similar modulus and  $\sigma_b$ , although 1,4-PBAF0.7 displayed a higher  $\epsilon_b$ .<sup>29</sup> Compared to the literature values, the recorded tensile properties of the PBAFs are low, which is expected because of their lower  $M_w$ s.<sup>37</sup>

In comparison to 2,5-PHAF0.7, 2,5-PHAF0.6 had much lower modulus and  $\sigma_b$  but higher  $\epsilon_b$ . This result was expected due to the reduced flexibility of the rigid furandioate unit in comparison to the aliphatic adipate unit. 2,5-PHAF0.6 samples extended to 500 mm (the instrument's maximum extension), at which point they were unbroken but extremely thin (Figure 5). The same occurred with samples of 1,4-PPAF0.7 and 2,7-POAF0.7. This is presumably a result of their entirely amorphous structures.

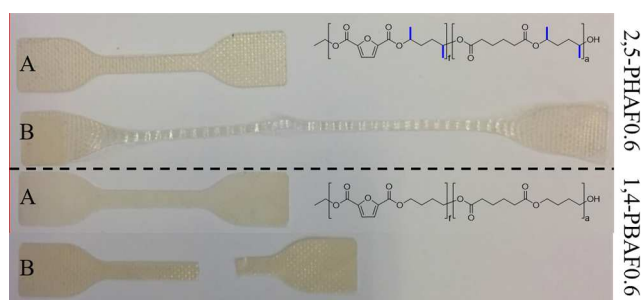


**Figure 5.** Photograph showing untested (A) and recovered tested (B) samples of 2,5-PHAF0.6 (top) and 1,4-PBAF0.6 (bottom) following tensile measurements.

2,7-POAF0.7 displayed the lowest modulus, 0.006 MPa, a value so low that it is likely to have been influenced by instrument limitations. The poor performance of this polymer is attributed primarily to a low chain length ( $M_w = 22$  kDa), though it could also be affected by having a larger  $D$  (2.9) compared to the other tested samples (1.5–1.8). This polymer was also the only material from the tensile strength study to have ester end groups confirmed by NMR analysis (22%), while all others were either confirmed to be solely –OH end groups or NMR analysis was inconclusive. 1,4-PPAF0.7 and 2,5-PHAF0.6 were both tough, rigid solids with appearances similar to that of 2,5-PHAF0.7, so it was surprising that they displayed such a low modulus and  $\sigma_b$ . The differences in tensile properties between 2,5-PHAF0.7 and the other samples of methyl-branched polyesters can be partially rationalized by  $T_g$  values and the fact that the measurements were recorded at room temperature (20–22 °C). 2,5-PHAF0.7 has a  $T_g$  (27 °C) just above room temperature, and so it was in its glassy state during measurement, whereas 2,5-PHAF0.6 (19 °C), 1,4-PPAF0.7 (12 °C), and 2,7-POAF0.7 (4 °C) have  $T_g$  values below room temperature, and thus were in their rubbery state during measurement. Although 1,4-PBAF0.7 and 1,6-PHAF0.7 were also in their rubbery states during measurement ( $T_g$  of –13 and –25 °C, respectively), both are also semicrystalline polymers that displayed higher modulus and  $\sigma_b$ . Evident from this study is that methyl branching of the diol clearly has an impact on material strength, allowing for the tuning of tensile properties, but that the concurrent influence on  $T_g$  also plays a significant role.

## ■ WATER CONTACT ANGLE MEASUREMENTS

The influence of methyl branches on the hydrophobicity of these copolyesters was evaluated from water contact angle (WCA) measurements (Table 3) using the sessile drop

**Table 3.** WCAs of All Polymers Tested<sup>a,b,d</sup>

entry	polymer	$M_w$ /kDa <sup>c</sup>	WCA/°C
1	1,4-PBAF0.5	28	83.0 ± 1.8
2	1,4-PBAF0.6	Nd	87.8 ± 4.7
3	1,4-PBAF0.7	Nd	103.6 ± 1.3
4	1,4-PPAF0.5	34	99.4 ± 2.8
5	1,4-PPAF0.6	29	88.4 ± 3.2
6	1,4-PPAF0.7	37	104.8 ± 4.4
7	2,5-PHAF0.5	24	95.8 ± 1.7
8	2,5-PHAF0.6	34	95.0 ± 3.3
9	2,5-PHAF0.7	22	112.3 ± 4.1
10 <sup>c</sup>	2,5-PHAF0.7 (low $M_w$ )	17	91.0 ± 6.2
11	1,6-PHAF0.5	Nd	78.5 ± 4.0
12	1,6-PHAF0.6	Nd	88.5 ± 3.1
13	1,6-PHAF0.7	Nd	93.2 ± 4.6
14	2,7-POAF0.5	57	106.9 ± 1.4
15	2,7-POAF0.6	39	100.9 ± 1.4
16	2,7-POAF0.7	21	96.9 ± 1.9

<sup>a</sup>Errors represent standard deviations. <sup>b</sup>Static measurements of the WCA using the sessile drop method at ambient temperature and pressure. Films were prepared as detailed in the Materials and Methods section; with use of a polyimide film a consistent smooth surface was produced. Droplets were allowed to stand for 10 s before being recorded for 3 s at a rate of 3 frames per second. Analysis was done using the Young–Laplace equation. At least five measurements were taken for drops in different areas of the film and their average and standard deviation were determined accordingly. <sup>c</sup>2,5-PBAF0.7 in entry 10 was prepared using a lower diol excess compared to entry 9 (optimized synthesis), resulting in a polyester with a lower  $M_n$  (12 kDa) and  $M_w$  (17 kDa). <sup>d</sup>Determined by GPC, nd shows samples not soluble in the GPC solvent (THF).

method on the films described above (Figure 6). Considering first the polyesters with no methyl branching (1,4-PBAFs entries 1–3 and 1,6-PHAFs entries 11–13), we note that increasing diol chain length resulted in a lower contact angle for like-for-like  $F/D$  ratios. Jiang *et al.* also observed this phenomenon when comparing the furan homopolymers 1,4-

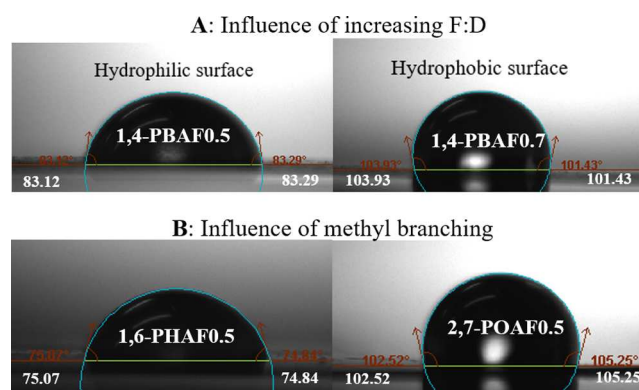


**Figure 6.** Examples of static WCA photographs demonstrating the (A) influence of increasing  $F/D$  over the 1,4-PBAF series and (B) influence of introducing methyl branching. Values shown are single points of data, while the values in Table 3 are averages of multiple static values.



PBF and 1,6-PHF, the latter being more hydrophilic.<sup>38</sup> One possible explanation for this is that the furandioate is the greater contributor to surface hydrophobicity and thus longer linear diols increase spacing between the furans. Indeed, Mathers' comprehensive study of functional group identity on polymer hydrophilicity does not necessarily follow an order of influence based on the simple C/O ratio.<sup>39</sup> Another possible reason is that 1,6-HDO is more likely to possess alcohol end groups as it does not easily form the cyclic ether byproduct during polycondensation, thus maintaining a higher OH to CO<sub>2</sub>Et end-group ratio. Mathers showed supporting evidence of the significant influence of polyester chain length on hydrophobicity when alcohol end groups are present, where shorter chains reduced hydrophobicity, and especially in cases with degrees of polymerization <8.<sup>39</sup>

As a general trend, hydrophobicity increased as *F/D* increased for both the methyl-branched and conventional linear furanate-adipate copolyesters. However, as Figure S73 shows, 1,4-PPAF0.6 and 2,5-PHAF0.6 were more hydrophilic than 1,4-PPAF0.5 and 2,5-PHAF0.5. Of note is that 2,5-PHAF0.5 had a markedly lower number of –OH end groups (38%, Table 1, entry 12) relative to 2,5-PHAF0.6 (all end groups were –OH). It is reasonable that a greater proportion of ester end groups will result in a more hydrophobic surface and would therefore explain the deviation in the trend seen for the 2,5-HDO series. The lower contact angle of 1,4-PPAF0.6 could be due to it having a lower *M<sub>w</sub>* than 1,4-PPAF0.5 (29 and 34 kDa, respectively), as a lower *M<sub>w</sub>* results in a greater number of hydrophilic OH end groups. This theory was confirmed by measuring the contact angle of low *M<sub>w</sub>* 2,5-PHAF0.7 (Table 3, entry 10, 91.0°, 17 kDa), which displayed

**Table 4. Optimum Polymerization Conditions for Each Polyester<sup>a</sup>**

polymer	Diol	diol/diester	<i>T</i> <sub>DEA ADD</sub> /h
1,4-PBAF	1,4-BDO	2:1	2
1,4-PPAF	1,4-PDO	2:1	4
2,5-PHAF	2,5-HDO	2:1	4
1,6-PHAF	1,6-HDO	1.25:1	2
2,7-POAF	2,7-ODO	2:1	4

<sup>a</sup>*T*<sub>DEA ADD</sub> = time that FDEE was left to react with diol before DEA was added.

lower hydrophobicity than that of a higher *M<sub>w</sub>* 2,5-PHAF0.7 (entry 9, 112.3°, 22 kDa). Another unexpected result was the decrease in hydrophobicity as the *F/D* ratio increased for the 2,7-POAF polyesters. Again, this was proposed to be a matter of *M<sub>w</sub>* as this dramatically decreases across this series. While no literature is available with which these values can be compared, the WCAs of 1,4-PBAFs and 1,6-PHAFs were expected to lie below the published values of the homopolymers 1,4-PBF (83.7°) and 1,6-PHF (80.4°).<sup>38</sup> Many of the values for the furandioate-adipate copolyesters were higher than this, possibly because of differences in experimental technique or *M<sub>w</sub>* and thus the influence of chain ends. Overall, these data strongly indicate that the addition of methyl branches from 2° alcohol diols increases the surface hydrophobicity in furandioate-adipate copolyesters. Of particular note is that the most hydrophobic material, 2,5-PBAF0.7, was also the best performing material in terms of modulus.

## ■ ENZYME-CATALYZED HYDROLYSIS

An initial study on the hydrolysis rates of 1,4-PBAF0.5, 1,4-PPAF0.5, and 2,5-PHAF0.5 was carried out to determine the timescale over which these polymers biodegrade and to show how methyl branching affects the rate. For these experiments, a commercial cutinase from *Humicola insolens* (HiC) was used as the biocatalyst as this was previously reported to efficiently hydrolyze both aliphatic and aromatic polyesters containing benzene and furan moieties.<sup>40–42</sup> Figure 7 shows that methyl

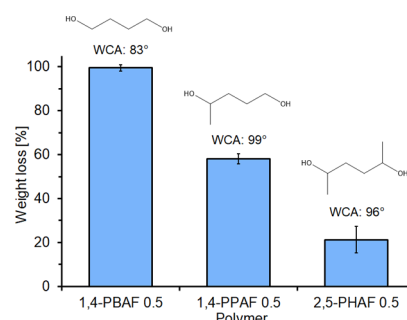


**Figure 7.** Weight loss of 1,4-PBAF0.5, 1,4-PPAF0.5, and 2,5-PHAF0.5 after 24 h of enzymatic degradation in 1 mL of 5  $\mu$ M *H. insolens* cutinase in 1 M KPO buffer at pH 8. All samples were run in triplicate alongside a blank reaction (buffer only) that showed no significant weight loss. Error bars represent the standard deviations of triplicate samples. WCA = water contact angle (see Table 3).

branching decreases the enzymatic hydrolysis rate. In fact, after 24 h of incubation with HiC, 1,4-PBAF0.5 was completely degraded into soluble compounds, while for the methyl-branched 1,4-PPAF0.5 (one methyl branch) and 2,5-PHAF0.5 (two methyl branches), the measured weight loss was 5 and 21%, respectively.

In order to better understand how the hydrolysis rate changes over time, additional hydrolysis studies using polymers containing a higher furandioate unit content (*F/D* = 0.7 for all) were undertaken. The enzymatic hydrolysis rates of 1,4-PBAF0.7, 2,5-PHAF0.7, 1,6-PHAF0.7, and 2,7-POAF0.7 were measured over a time course reaction. Using copolymers containing a higher furandioate unit content enabled the rates to be examined over 48 h. As Figure 8 shows, this study confirmed that the rate of enzymatic hydrolysis was slowed by

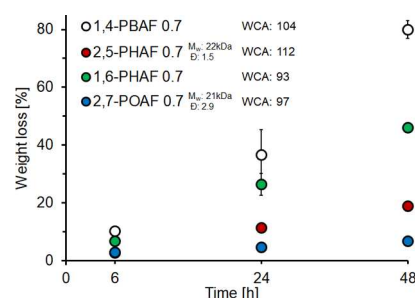


**Figure 8.** Weight loss of 1,4-PBAF0.7, 2,5-PHAF0.7, 1,6-PHAF, and 2,7-POAF0.7 over a 48 h time course enzymatic degradation in 1 mL of 5  $\mu$ M *H. insolens* cutinase in 1 M KPO buffer at pH 8, 65 °C. All samples were run in triplicate alongside the blank reaction (buffer only) that showed no significant weight loss. Error bars represent the standard deviations of triplicate samples, and those with no error bars had standard deviations that were too small to display. WCA = water contact angle.

methyl branching in both sets of polymers (1,4-PBAF0.7 and 1,6-PHAF0.7). It was also observed that, for the polymers analyzed, longer chain polyesters had lower rates of enzymatic hydrolysis. After 48 h, 1,4-PBAF0.7 showed a weight loss of 80%, whereas 2,5-PHAF0.7 had only 19% weight loss. Likewise, 1,6-PHAF0.7 displayed 46% weight loss after 48 h, while 2,7-POAF0.7 showed only 7% weight loss.

As shown by their lack of  $T_m$ , the methyl-branched 1,4-PPAF and 2,5-PHAF polymers are entirely amorphous, whereas the 1,4-PBAFs are semicrystalline. As enzymes typically preferentially degrade the amorphous regions of a polyester,<sup>43–45</sup> the more crystalline 1,4-PBAFs were anticipated to degrade more slowly than their methyl-branched analogues. However, this was not the case, and methyl branching was seen to be a significant factor in the enzyme hydrolysis rate. We expected that the rate of hydrolysis might also be linked to the surface energy, with the more hydrophobic surfaces being slower to hydrolyze. A closer inspection of the relationship between WCA (values next to series legends in Figure 8) and the rate of enzymatic hydrolysis instead suggests that the hydrolytic stability seen for the 2,5-PHAF0.7 and 2,7-POAF0.7 polyesters was predominately a result of steric hindrance around the ester bonds in the polymer backbone. Based on the WCA alone, we would have predicted the order of enzyme hydrolytic stability to be 2,5-PHAF0.7 > 1,4-PBAF0.7 > 2,7-POAF0.7 > 1,6-PHAF0.7, yet the order clearly shows the methyl-branched polyesters to be significantly more resilient to hydrolysis. An explicit reason for the slower degradation could therefore be that methyl branching sterically encumbers the ester group, reducing the degree of interaction with the enzyme's active site. In fact, when using *Candida antarctica* lipase B as the catalyst for transesterification, low degrees of polymerization (leading to only short oligomers) were observed when attempting to synthesize 2,5-PHA and 2,7-POA (Table S10 for the complete set of data on enzymatic polymerization of methyl-branched diols). These data are fully supported by previous reports on the inhibition of esterification of 2° and tertiary alcohols with enzymes belonging to the serin-hydrolase family.<sup>46,47</sup> It is also known that the enzymatic hydrolysis of aliphatic polyesters such as PLA<sup>48</sup> and PBS<sup>49</sup> is usually faster than the degradation of aromatic–aliphatic polyesters such as PBAT<sup>50</sup> and aromatic polyesters such as PET.<sup>51,52</sup> This indicates that steric hindrance derived from the monomers has a greater impact than crystallinity on the enzymatic degradation of these materials, although further studies would be needed to confirm this. For example, the significant shift in  $T_g$  from the aliphatic polyesters to the aromatic-containing polyesters makes direct comparisons challenging, while the aliphatic polyester PLA has a relatively slow rate of hydrolysis because of its high  $T_g$  and semicrystalline character.

As it is known that  $M_w$  greatly impacts the rate of biodegradation, it is important to ensure that the samples being tested were of similar  $M_w$ . GPC analysis confirmed 1,4-PBAF0.5, 1,4-PPAF0.5, and 2,5-PHAF0.5 all to be of comparable  $M_w$  and  $M_n$  (Table 1). While the rate of enzymatic hydrolysis typically decreases with increasing  $M_w$ , differences in chain length can be discounted from affecting the observed trends. During the hydrolysis studies, a few hours after incubation, all film samples of the methyl-branched copolyesters from 2° diols lost their shape, turning from flat 0.5 × 1.0 cm rectangles into beads (Figure 9). These tests were carried out at 65 °C, well above the  $T_g$  values of all the polymers. As

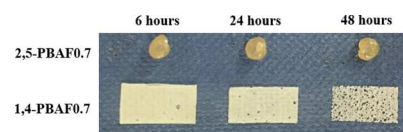


**Figure 9.** Enzymatic degradation samples of 2,5-PHAF0.7 (top) and 1,4-PBAF0.7 (bottom) after 6 h (left), 24 h (middle), and 48 h (right). Reaction conditions: 65 °C, 1 mL of 5  $\mu$ M *H. insolens* cutinase in 1 M KPO buffer at pH 8. All samples started as 0.5 × 1.0 cm<sup>2</sup> rectangles.

the methyl-branched polymers were entirely amorphous (no  $T_m$  observed in DSC), they were soft and deformable at this temperature. Combining this with their high hydrophobicity, the samples formed spheres in order to reduce their surface area in contact with the aqueous buffer solution. This impacted the hydrolysis data, as a lower surface area sample has less contact with the enzyme, resulting in a lower degradation rate.

It is clear from these results that both methyl branching and a higher furan content in the polymer chain reduced the rate of enzyme hydrolysis in furandioate-adipate copolyesters. This study thus demonstrates that the use of methyl-branched diols is an effective means in improving the hydrolytic stability of a polyester, a benefit in applications where the service lifetime of a plastic needs to be long, or for hydrolytically more stable coatings and surfaces.

## MATERIALS AND METHODS

1,4-Butanediol (1,4-BDO), 2,3-butanediol (2,3-BDO), 1,4-pentane-1,4-diol (1,4-PDO), 1,6-hexanediol (1,6-HDO), 2,5-hexanediol (2,5-HDO), diethyl adipate (DEA), levulinic acid, titanium isopropoxide (Ti(O<sup>i</sup>Pr)<sub>4</sub>), buffer solutions, THF (analytical grade, degassed), ReadyCal polystyrene standards, tetradecane standard, and deuterated chloroform (CDCl<sub>3</sub>) were purchased from Sigma-Aldrich and used as received. 2,5-Furandicarboxylic acid diethyl ester (FDEE, >99%) was purchased from Carbosynth and used as received. Cutinase from *H. insolens* (HiC) was purchased from Strem Chemicals and stored under vacuum following lyophilization. 10% Pd/C and La(OTf)<sub>3</sub> were purchased from Strem Chemicals. 2,7-Octanediol (2,7-ODO) was prepared using a previously reported method.<sup>2</sup> Diols were dried over molecular sieves prior to use in polymerizations. A Kapton HN polyimide sheet (Dupont) was used between the heated plates and samples for pressing films for WCA measurements.

**1° Alcohol Conditions: Preparation of Copolyesters from 1° Alcohol Diols.** A mixture of diol (12.5 mmol), FDEE (total diester feed of 10 mmol) and Ti(O<sup>i</sup>Pr)<sub>4</sub> (1 mol % relative to total diester) was introduced into a 25 mL wide-neck round-bottom flask equipped with a stirrer bar. This was attached to a Dean–Stark condenser and a Schlenk line. The system was evacuated and back-filled with argon/nitrogen four times, heated to 150 °C, and stirred at 300 rpm. After 2 h, DEA (total diester was 10 mmol) was added. After a further 2 h, the temperature was increased to 180 °C. The distillate was collected from the Dean–Stark trap a further hour into the experiment and the pressure was reduced to 200 mbar. After ~15 h, the pressure was further reduced to 4 mbar, and 30 min later full vacuum was applied (<1 mbar). The stirring rate was then reduced as the mixture thickened. After a further 4 h, the system was back-filled with argon/nitrogen and the polymer was removed while in the molten state. The polymer samples were analyzed as collected.

**2° Alcohol Optimized Conditions: Preparation of Copolyesters from 2° Alcohol Diols.** A mixture of diol (20 mmol), FDEE (total diester was 10 mmol), and Ti(O<sup>i</sup>Pr)<sub>4</sub> (1 mol % relative to total diester) was introduced into a wide-neck round-bottom flask equipped with a stirrer bar. This was attached to a Dean–Stark condenser and a Schlenk line. The system was evacuated and back-filled with argon/nitrogen four times, heated to 150 °C, and stirred at 300 rpm. After 4 h, DEA (total diester was 10 mmol) was added and

after a further 2 h, the temperature was raised to 180 °C. The distillate was collected from the Dean–Stark trap a further hour (7 h total) into the experiment and the pressure was reduced to 200 mbar. After another ~15 h, the pressure was further reduced to 4 mbar, and 30 min later full vacuum was applied (<1 mbar). The stirring rate was reduced as the mixture thickened. The reaction was performed until the Weissenberg effect emerged (4–7 h later). The system was then back-filled with argon/nitrogen and the polymer was removed while in the molten state. The polymer samples were analyzed as collected.

**Optimized Procedure for the Preparation of Homopolyesters.** A mixture of diol (12.5 mmol using DEA) (20.0 mmol using FDEE), diester (total 10 mmol), and  $\text{Ti}(\text{O}^i\text{Pr})_4$  (1 mol % relative to total diester) was introduced into a wide-neck round-bottom flask equipped with a stirrer bar. This was attached to a Dean–Stark condenser and a Schlenk line. The system was evacuated and back-filled with argon/nitrogen four times, heated to 150 °C, and stirred at 300 rpm. After 2 h, the temperature was raised to 180 °C. The distillate was collected from the Dean–Stark trap a further hour into the experiment and the pressure was reduced to 200 mbar. After another ~15 h, the pressure was further reduced to 4 mbar, and 30 min later full vacuum was applied (<1 mbar). The stirring rate was then reduced as the mixture thickened. The reaction was performed until the Weissenberg effect emerged (4–7 h later). The system was then back-filled with argon/nitrogen and the polymer was removed while in a molten state. When using 2° diols, the system was left for 3–4 h at the initial 150 °C before increasing the temperature to 180 °C. The polymer samples were analyzed as collected.

**$^1\text{H}$  NMR Spectroscopy.** NMR spectra were obtained on a Jeol 400 spectrometer (400 MHz) using  $\text{CDCl}_3$  as a solvent and TMS as the internal standard. Samples were prepared by dissolving 10–20 mg of sample in  $\text{CDCl}_3$ .

**Gel Permeation Chromatography.** GPC was carried out using a set (PSS SDV High) of three analytical columns (300 × 8 mm, particle diameter: 5  $\mu\text{m}$ ) of 1000, 105, and 106 Å pore sizes and a guard column, supplied by Polymer Standards Service GmbH (PSS) installed in a PSS SECurity SEC system. Elution was with THF at 1 mL/min at a column temperature of 30 °C and detection was done by refractive index. 20  $\mu\text{L}$  of a 1 mg/mL sample in THF, with a small quantity of toluene added as a flow marker, was injected for each measurement and eluted for 45 min. Calibration was carried out in the molecular weight range 400 to  $2 \times 10^6$  Da using ReadyCal polystyrene standards (Sigma Aldrich) and referenced to the toluene peak.

**Differential Scanning Calorimetry.** DSC experiments were performed on a TA Instruments Q2000 DSC. Samples were scanned under a nitrogen atmosphere over a temperature range of –80 to 200 °C and at a heating rate of 10 °C  $\text{min}^{-1}$ . Samples of mass ~10 mg were used.  $T_g$  values were reported from the second heating scans.

**Film Preparation of Polyesters.** Films were prepared using a hot-press. Samples were placed between Teflon sheets and plates were positioned on either side of the polymer (~4 cm apart). Polymers prepared from 1,4-PDO, 2,5-HDO, and 2,7-ODO were heated to 100 °C and then pressed for 30 s at 10 tonnes. Polymers prepared from 1,4-BDO and 1,6-HDO were heated to 150 °C and then pressed at 1 tonne for 10 s. Films of a thickness of  $0.30 \pm 0.03$  mm were obtained. The reported thickness (Table S9) represents the mean of 10 measurements taken using a micrometer at different points of the polymer film. For the contact angle measurements, films were prepared using a polyimide film (bottom layer) and a smooth Teflon film (top layer). The Teflon film was removed just before taking measurements.

**Tensile Measurements of Polyesters.** Tensile properties were measured using an Instron 3367 machine. Dumbbell-shaped specimens 0.3 mm in thickness (the thickness range is available in Table S9), 20 mm in length, and 3 mm in width with a  $10 \times 10$  mm square for gripping at each end were punched from the prepared films. Samples were tested at a rate of 5 mm/min at ambient temperature and pressure using screw action rubber grip claws and a 100 N (max) static load cell. For each sample, at least four specimens were tested.

**Enzyme-Catalyzed Hydrolysis of Polyester Films.** This was done based on a previously reported method.<sup>45,49</sup> Consistent  $0.5 \times 1.0$  cm pieces were cut from 0.3 mm deep films, washed to remove surface impurities (5 g/L Triton X-100, 100 mM  $\text{Na}_2\text{CO}_3$ , and deionized  $\text{H}_2\text{O}$ , each for 30 min at RTP), and dried overnight in a vacuum oven. The film pieces were then weighed, placed in a weighed 2 mL Eppendorf tube, and incubated with 1.0 mL of 5  $\mu\text{M}$  *H. insolens* cutinase (HiC) in a 1 M pH 8  $\text{KH}_2\text{PO}_4/\text{K}_2\text{HPO}_4$  buffer solution. Incubation was carried out in an Eppendorf ThermoMixer at 65 °C and 300 rpm. After the required time, samples were removed, washed repeatedly with deionized water, dried in a vacuum oven overnight, and weighed. All samples were run in triplicate alongside a blank (incubated as stated but without the HiC). The degradation rate was calculated from the weight loss using eq 1

$$W = \frac{m_0 - m_1}{m_0} \times 100\% \quad (1)$$

where  $W$  is the weight loss/%,  $m_0$  is the mass before/g, and  $m_1$  is the mass after/g.

**WCA Measurements of Films.** Static measurements of the WCA were performed on an Attension ThetaLite101 goniometer using the sessile drop method at RTP. The water droplets were allowed to stand for 10 s before being recorded for 3 s at a rate of 3 frames per second. Analysis was performed using the Young–Laplace equation. At least five measurements were taken of drops in different areas of the film and their average and standard deviation were recorded.

## CONCLUSIONS

High  $M_w$  (>20 kDa) furandioate-adipate copolyesters from 2° alcohol diols (1,4-PDO, 2,5-HDO, and 2,7-ODO) with a furan/adipate molar ratio in the 0.5–0.7 range were synthesized via melt polycondensation using  $\text{Ti}(\text{O}^i\text{Pr})_4$  as the catalyst. Loss of diol to oxolane formation prevented the formation of high  $M_w$  copolyesters in some cases. Increasing the diol/diester load ratio from 1.25:1 to 2:1 partially overcame this issue.

For the first time, the mechanical properties, hydrolytic stability, and WCA of methyl-branched copolyesters from bio-based 2° diols (1,4-PPAF, 2,5-PHAF, and 2,7-POAF) could be compared to their linear equivalents from 1° diols (1,4-PBAF and 1,6-PHAF). As has been previously observed, methyl-branched copolyesters displayed higher  $T_g$ s than their equivalents from 1° alcohol diols. As expected, across the series,  $T_g$  increased with increasing furandioate unit content. All copolyesters from 2° diols were entirely amorphous (displayed no melting points by DSC) whereas those from 1° diols were semicrystalline (distinct melting points detected). This reduced crystallinity gave these methyl-branched polymers increased flexibility (higher extension at break), indicating easier processability. Methyl-branched 2,5-PHAF0.7 displayed a modulus three times that of 1,4-PBAF0.7 (67.8 MPa vs 19.1 MPa, respectively), thus comprising a stiffer material. In apparent contradiction to this, the methyl-branched polyester also showed a far superior extension at break (89.7 vs 44.5 mm), indicative of a more flexible material. The high modulus of 2,5-PHAF0.7 in comparison to the low modulus of all other methyl-branched materials is attributed to differences in  $T_g$ , with 2,5-PHAF0.7 being only copolyester to have a  $T_g$  (27 °C) above the test temperature. WCA measurements revealed that the methyl-branched copolyesters were generally more hydrophobic than their linear 1° alcohol diol equivalents, with some influence of alcohol end groups also observed. *H. insolens* cutinase-catalyzed ester hydrolysis studies showed that methyl branching slows the rate of enzymatic hydrolysis, indicating slower biodegradation (on the



order of 5 times after 24 h of incubation for 1,4-PBAF vs 2,5-PHAF) and thereby a longer service life for materials that would benefit from greater robustness. Steric influence around the ester appears to be the major contributing factor to the marked difference in behavior between these polyesters.

In conclusion, 100% bio-based copolyesters of methyl-branched diols are shown to have great potential both in terms of material performance (thermomechanical and water resistance) and the ability to tune their useful service life where this may be a commercial advantage, such as uses in coatings.

## ■ ASSOCIATED CONTENT

### ■ Supporting Information

The Supporting Information is available free of charge at <https://pubs.acs.org/doi/10.1021/acssuschemeng.0c04513>.

Preliminary investigation of suitable conditions of synthesis of furandioate-adipate copolyesters with 2,5-HDO, analysis of distillate collected during polycondensation, <sup>1</sup>H NMR spectra, GPC chromatograms, tabulated literature values for GPC and DSC analysis, DSC analysis, photographs of polyester samples, film thickness, tensile analysis of polyester films, graph of trends in WCA and furan content, and polyester synthesis using CaLB enzyme as a catalyst (PDF)

## ■ AUTHOR INFORMATION

### Corresponding Authors

**Mark Mascal** – Department of Chemistry, University of California Davis, Davis, California 95616, United States; [orcid.org/0000-0001-7841-253X](https://orcid.org/0000-0001-7841-253X); Email: [mjmascal@ucdavis.edu](mailto:mjmascal@ucdavis.edu)

**Thomas J. Farmer** – Green Chemistry Centre of Excellence, Department of Chemistry, University of York, York YO10 SDD, U.K.; [orcid.org/0000-0002-1039-7684](https://orcid.org/0000-0002-1039-7684); Email: [thomas.farmer@york.ac.uk](mailto:thomas.farmer@york.ac.uk)

### Authors

**Alastair Little** – Green Chemistry Centre of Excellence, Department of Chemistry, University of York, York YO10 SDD, U.K.

**Alessandro Pellis** – Green Chemistry Centre of Excellence, Department of Chemistry, University of York, York YO10 SDD, U.K.; Department of Agrobiotechnology, Institute of Environmental Biotechnology, University of Natural Resources and Life Sciences, Vienna, Tulln an der Donau 3430, Austria; [orcid.org/0000-0003-3711-3087](https://orcid.org/0000-0003-3711-3087)

**James W. Comerford** – Green Chemistry Centre of Excellence, Department of Chemistry, University of York, York YO10 SDD, U.K.; [orcid.org/0000-0002-9977-5695](https://orcid.org/0000-0002-9977-5695)

**Edwin Naranjo-Valles** – Department of Chemistry, University of California Davis, Davis, California 95616, United States

**Nema Hafezi** – Department of Chemistry, University of California Davis, Davis, California 95616, United States

Complete contact information is available at:

<https://pubs.acs.org/doi/10.1021/acssuschemeng.0c04513>

### Author Contributions

The manuscript was written through contributions of all authors. All authors have given approval to the final version of the manuscript.

### Funding

T.J.F. and J.W.C. thank the UK Engineering and Physical Sciences Research Council (EPSRC, grant EP/L017393/1) and the Biotechnology and Biological Sciences Research Council (BBSRC, grant BB/N023595/1) for supporting their involvement in this study. A.P. thanks the FWF Erwin Schrödinger fellowship (grant agreement J 4014-N34) for financial support.

### Notes

The authors declare no competing financial interest.

Raw data gathered from the work supported by grants EP/L017393/1 and BB/BB/N023595/1 are available in the Supporting Information or available via DOI: [10.15124/2d8cdd51-69a4-4fb4-a7e3-f7e92ab073ca](https://doi.org/10.15124/2d8cdd51-69a4-4fb4-a7e3-f7e92ab073ca).

## ■ REFERENCES

- (1) Arnaud, S. P.; Wu, L.; Wong Chang, M.-A.; Comerford, J. W.; Farmer, T. J.; Schmid, M.; Chang, F.; Li, Z.; Mascal, M. New bio-based monomers: tuneable polyester properties using branched diols from biomass. *Faraday Discuss.* **2017**, *202*, 61–77.
- (2) Wu, L.; Mascal, M.; Farmer, T. J.; Arnaud, S. P.; Wong Chang, M.-A. Electrochemical coupling of biomass-derived acids: New C8 platforms for renewable polymers and fuels. *ChemSusChem* **2017**, *10*, 166–170.
- (3) Mascal, M.; Nikitin, E. B. High-yield conversion of plant biomass into the key value-added feedstocks 5-(hydroxymethyl)furfural, levulinic acid, and levulinic esters via 5-(chloromethyl)furfural. *Green Chem.* **2010**, *12*, 370–373.
- (4) Laugel, C.; Estrine, B.; Le Bras, J.; Hoffmann, N.; Marinkovic, S.; Muzart, J. NaBr/DMSO-induced synthesis of 2,5-diformylfuran from fructose or 5-(hydroxymethyl)furfural. *Chemcatchem* **2014**, *6*, 1195–1198.
- (5) Dutta, S.; Mascal, M. Novel pathways to 2,5-dimethylfuran via biomass-derived 5-(chloromethyl)furfural. *ChemSusChem* **2014**, *7*, 3028–3030.
- (6) Dutta, S.; Wu, L.; Mascal, M. Efficient, metal-free production of succinic acid by oxidation of biomass-derived levulinic acid with hydrogen peroxide. *Green Chem.* **2015**, *17*, 2335–2338.
- (7) Creusen, G.; Holzhäuser, F. J.; Artz, J.; Palkovits, S.; Palkovits, R. Producing widespread monomers from biomass using economical carbon and ruthenium-titanium dioxide electrocatalysts. *ACS Sustainable Chem. Eng.* **2018**, *6*, 17108–17113.
- (8) Dutta, S.; Wu, L.; Mascal, M. Production of 5-(chloromethyl)-furan-2-carbonyl chloride and furan-2,5-dicarbonyl chloride from biomass-derived 5-(chloromethyl)furfural (CMF). *Green Chem.* **2015**, *17*, 3737–3739.
- (9) Li, Y.; Lv, G.; Wang, Y.; Deng, T.; Wang, Y.; Hou, X.; Yang, Y. Synthesis of 2,5-hexanedione from biomass resources using a highly efficient biphasic system. *Chemistryselect* **2016**, *1*, 1252–1255.
- (10) Latifi, E.; Marchese, A. D.; Hulls, M. C. W.; Soldatov, D. V.; Schlaf, M. [Ru(triphos)(CH<sub>3</sub>CN)(3)](OTf)(2) as a homogeneous catalyst for the hydrogenation of biomass derived 2,5-hexanedione and 2,5-dimethyl-furan in aqueous acidic medium. *Green Chem.* **2017**, *19*, 4666–4679.
- (11) Yu, X.; Jia, J.; Xu, S.; Lao, K. U.; Sanford, M. J.; Ramakrishnan, R. K.; Nazarenko, S. I.; Hoye, T. R.; Coates, G. W.; DiStasio, R. A., Jr. Unraveling substituent effects on the glass transition temperatures of biorenewable polyesters. *Nat. Commun.* **2018**, *9*, 2880.
- (12) Sullivan, R. J.; Latifi, E.; Chung, B. K.-M.; Soldatov, D. V.; Schlaf, M. Hydrodeoxygenation of 2,5-hexanedione and 2,5-dimethylfuran by water-, air-, and acid-stable homogeneous ruthenium and iridium catalysts. *ACS Catal.* **2014**, *4*, 4116–4128.
- (13) Boyd, R. H.; Aylwin, P. A. Aliphatic polyesters as models for relaxation processes in crystalline polymers. 2. Dielectric-relaxation in copolymers of adipic Acid with 1,6 and 2,5-hexanediols. *Polymer* **1984**, *25*, 330–339.



- (14) van der Klis, F.; Knoop, R. J. I.; Bitter, J. H.; van den Broek, L. A. M. The effect of Me-substituents of 1,4-butanediol analogues on the thermal properties of biobased polyesters. *J. Polym. Sci., Part A: Polym. Chem.* **2018**, *56*, 1903–1906.
- (15) Ortner, A.; Pellis, A.; Gamerith, C.; Orcal Yebra, A.; Scaini, D.; Kaluzna, I.; Mink, D.; de Wildeman, S.; Herrero Acero, E.; Guebitz, G. M. Superhydrophobic functionalization of cutinase activated poly(lactic acid) surfaces. *Green Chem.* **2017**, *19*, 816–822.
- (16) Gao, A.; Zhao, Y.; Yang, Q.; Fu, Y.; Xue, L. Facile preparation of patterned petal-like PLA surfaces with tunable water micro-droplet adhesion properties based on stereo-complex co-crystallization from non-solvent induced phase separation processes. *J. Mater. Chem. A* **2016**, *4*, 12058–12064.
- (17) Bérard, A.; Patience, G. S.; Chouinard, G.; Tavares, J. R. Photo initiated chemical vapour deposition to increase polymer hydrophobicity. *Sci. Rep.* **2016**, *6*, 31574.
- (18) Knoch, S.; Chouinard, G.; Dumont, M.-J.; Tavares, J. R. Dip-dip-dry: Solvent-induced tuning of polylactic acid surface properties. *Colloids Surf., A* **2019**, *578*, 123591.
- (19) Gubbels, E.; Jasinska-Walc, L.; Koning, C. E. Synthesis and characterization of novel renewable polyesters based on 2,5-furandicarboxylic acid and 2,3-butanediol. *J. Polym. Sci., Part A: Polym. Chem.* **2013**, *51*, 890–898.
- (20) Thiagarajan, S.; Vogelzang, W.; Knoop, R. J. I.; Frissen, A. E.; van Haveren, J.; van Es, D. S. Biobased furandicarboxylic acids (FDCA): effects of isomeric substitution on polyester synthesis and properties. *Green Chem.* **2014**, *16*, 1957–1966.
- (21) Fenouillot, F.; Rousseau, A.; Colomines, G.; Saint-Loup, R.; Pascault, J.-P. Polymers from renewable 1,4:3,6-dianhydrohexitols (isosorbide, isomannide and isoidide): A review. *Prog. Polym. Sci.* **2010**, *35*, 578–622.
- (22) Saxon, D. J.; Luke, A. M.; Sajjad, H.; Tolman, W. B.; Reineke, T. M. Next-generation polymers: Isosorbide as a renewable alternative. *Prog. Polym. Sci.* **2020**, *101*, 101196.
- (23) Lomeli-Rodríguez, M.; Corpas-Martínez, J.; Willis, S.; Mulholland, R.; Lopez-Sanchez, J. Synthesis and characterization of renewable polyester coil coatings from biomass-derived isosorbide, FDCA, 1,5-pentanediol, succinic acid, and 1,3-propanediol. *Polymers* **2018**, *10*, 600.
- (24) Haernvall, K.; Zitzenbacher, S.; Amer, H.; Zumstein, M. T.; Sander, M.; McNeill, K.; Yamamoto, M.; Schick, M. B.; Ribitsch, D.; Guebitz, G. M. Polyol structure influences enzymatic hydrolysis of bio-based 2,5-furandicarboxylic acid (FDCA) polyesters. *Biotechnol. J.* **2017**, *12*, 1600741.
- (25) Ejlertsson, J.; Alnervik, M.; Jonsson, S.; Svensson, B. H. Influence of water solubility, side-chain degradability, and side-chain structure on the degradation of phthalic acid esters under methanogenic conditions. *Environ. Sci. Technol.* **1997**, *31*, 2761–2764.
- (26) Genovese, L.; Lotti, N.; Siracusa, V.; Munari, A. Poly(neopentyl glycol furanoate): A member of the furan-based polyester family with smart barrier performances for sustainable food packaging applications. *Materials* **2017**, *10*, 1028.
- (27) Guidotti, G.; Soccio, M.; Siracusa, V.; Gazzano, M.; Salattelli, E.; Munari, A.; Lotti, N. Novel random PBS-based copolymers containing aliphatic side chains for sustainable flexible food packaging. *Polymers* **2017**, *9*, 724.
- (28) Peng, S. B.; Wu, L. B.; Li, B. G.; Dubois, P. Hydrolytic and compost degradation of biobased PBSF and PBAF copolymers with 40–60 mol% BF unit. *Polym. Degrad. Stab.* **2017**, *146*, 223–228.
- (29) Wu, B.; Xu, Y.; Bu, Z.; Wu, L.; Li, B.-G.; Dubois, P. Biobased poly(butylene 2,5-furandicarboxylate) and poly(butylene adipate-co-butylene 2,5-furandicarboxylate)s: From synthesis using highly purified 2,5-furandicarboxylic acid to thermo-mechanical properties. *Polymer* **2014**, *55*, 3648–3655.
- (30) de With, G. *Polymer Coatings: A Guide to Chemistry, Characterization, and Selected Applications*, 1st ed.; Wiley-VCH: Germany, Weinheim, 2018.
- (31) Raju, K. V. S. N.; Chattopadhyay, D. K., Chapter 9: Polyester Coatings for Corrosion Protection. In *High-Performance Organic Coatings*, 1st ed.; Khanna, A. S., Ed.; Woodhead Publishing: Cambridge, England, 2008; pp 165–200.
- (32) Gan, Z.; Kuwabara, K.; Yamamoto, M.; Abe, H.; Doi, Y. Solid-state structures and thermal properties of aliphatic-aromatic poly-(butylene adipate-co-butylene terephthalate) copolymers. *Polym. Degrad. Stab.* **2004**, *83*, 289–300.
- (33) Wu, L.; Mincheva, R.; Xu, Y.; Raquez, J.-M.; Dubois, P. High molecular weight poly(butylene succinate-co-butylene furandicarboxylate) copolymers: From catalyzed polycondensation reaction to thermomechanical properties. *Biomacromolecules* **2012**, *13*, 2973–2981.
- (34) Hunt, A. J.; Farmer, T. J.; Clark, J. H., Chapter 1: Elemental Sustainability and the Importance of Scarce Element Recovery. In *Element Recovery and Sustainability*, 1st ed.; Hunt, A. J., Ed.; The Royal Society of Chemistry: Cambridge, U.K., 2013; pp 1–28.
- (35) Zhu, J.; Cai, J.; Xie, W.; Chen, P.-H.; Gazzano, M.; Scandola, M.; Gross, R. A. Poly(butylene 2,5-furan dicarboxylate), a biobased alternative to PBT: Synthesis, physical properties, and crystal structure. *Macromolecules* **2013**, *46*, 796–804.
- (36) Farmer, T.; Castle, R.; Clark, J.; Macquarrie, D. Synthesis of unsaturated polyester resins from various bio-derived platform molecules. *Int. J. Mol. Sci.* **2015**, *16*, 14912–14932.
- (37) Xie, H.; Wu, L.; Li, B.-G.; Dubois, P. Biobased poly(ethylene-co-hexamethylene 2,5-furandicarboxylate) (PEHF) copolymers with superior tensile properties. *Ind. Eng. Chem. Res.* **2018**, *57*, 13094–13102.
- (38) Jiang, M.; Liu, Q.; Zhang, Q.; Ye, C.; Zhou, G. A series of furan-aromatic polyesters synthesized via direct esterification method based on renewable resources. *J. Polym. Sci., Part A: Polym. Chem.* **2012**, *50*, 1026–1036.
- (39) Dharmaratne, N. U.; Jouaneh, T. M. M.; Kiesewetter, M. K.; Mathers, R. T. Quantitative measurements of polymer hydrophobicity based on functional group identity and oligomer length. *Macromolecules* **2018**, *51*, 8461–8468.
- (40) de Castro, A. M.; Carniel, A.; Nicomedes Junior, J.; da Conceição Gomes, A.; Valoni, E. Screening of commercial enzymes for poly(ethylene terephthalate) (PET) hydrolysis and synergy studies on different substrate sources. *J. Ind. Microbiol. Biotechnol.* **2017**, *44*, 835–844.
- (41) Kawai, F.; Kawabata, T.; Oda, M. Current knowledge on enzymatic PET degradation and its possible application to waste stream management and other fields. *Appl. Microbiol. Biotechnol.* **2019**, *103*, 4253–4268.
- (42) Pellis, A.; Haernvall, K.; Pichler, C. M.; Ghazaryan, G.; Breinbauer, R.; Guebitz, G. M. Enzymatic hydrolysis of poly(ethylene furanoate). *J. Biotechnol.* **2016**, *235*, 47–53.
- (43) Mochizuki, M.; Hirami, M. Structural effects on the biodegradation of aliphatic polyesters. *Polym. Adv. Technol.* **1997**, *8*, 203–209.
- (44) Mueller, R.-J. Biological degradation of synthetic polyesters - enzymes as potential catalysts for polyester recycling. *Process Biochem.* **2006**, *41*, 2124–2128.
- (45) Weinberger, S.; Haernvall, K.; Scaini, D.; Ghazaryan, G.; Zumstein, M. T.; Sander, M.; Pellis, A.; Guebitz, G. M. Enzymatic surface hydrolysis of poly(ethylene furanoate) thin films of various crystallinities. *Green Chem.* **2017**, *19*, 5381–5384.
- (46) Stamatis, H.; Xenakis, A.; Provelegiou, M.; Kolisis, F. N. Esterification reactions catalyzed by lipases in microemulsions - the role of enzyme localization in relation to its selectivity. *Biotechnol. Bioeng.* **1993**, *42*, 103–110.
- (47) Cha, H.-J.; Park, J.-B.; Park, S. Esterification of secondary alcohols and multi-hydroxyl compounds by *Candida antarctica* lipase B and subtilisin. *Biotechnol. Bioprocess Eng.* **2019**, *24*, 41–47.
- (48) Pellis, A.; Acero, E. H.; Weber, H.; Obersiebnig, M.; Breinbauer, R.; Srebotnik, E.; Guebitz, G. M. Biocatalyzed approach for the surface functionalization of poly(L-lactic acid) films using hydrolytic enzymes. *Biotechnol. J.* **2015**, *10*, 1739–1749.
- (49) Gamerith, C.; Vastano, M.; Ghorbanpour, S. M.; Zitzenbacher, S.; Ribitsch, D.; Zumstein, M. T.; Sander, M.; Herrero Acero, E.;

Pellis, A.; Guebitz, G. M. Enzymatic degradation of aromatic and aliphatic polyesters by *P. pastoris* expressed cutinase 1 from *Thermobifida cellulosilytica*. *Front. Microbiol.* **2017**, *8*, 938.

(50) Perz, V.; Bleymaier, K.; Sinkel, C.; Kueper, U.; Bonnekessel, M.; Ribitsch, D.; Guebitz, G. M. Data on synthesis of oligomeric and polymeric poly(butylene adipate-co-butylene terephthalate) model substrates for the investigation of enzymatic hydrolysis. *Data Brief.* **2016**, *7*, 291–298.

(51) Quartinello, F.; Vajnhandl, S.; Volmajer Valh, J.; Farmer, T. J.; Vončina, B.; Lobnik, A.; Herrero Acero, E.; Pellis, A.; Guebitz, G. M. Synergistic chemo-enzymatic hydrolysis of poly(ethylene terephthalate) from textile waste. *Microb. Biotechnol.* **2017**, *10*, 1376–1383.

(52) Gamerith, C.; Zartl, B.; Pellis, A.; Guillaumot, F.; Marty, A.; Acero, E. H.; Guebitz, G. M. Enzymatic recovery of polyester building blocks from polymer blends. *Process Biochem.* **2017**, *59*, 58–64.